A Flexible OLED VLC System for an Office Environment

Zahra Nazari Chaleshtori[1], Stanislav Zvanovec[1], Zabih Ghassemlooy[2], Hossien B. Eldeeb[3] and Murat Uysal[3]

[1]*Deptartment of Electromagnetic Field, Faculty of Electrical Engineering, Czech Technical University in Prague, Prague, Czech Republic, 16627.*

[2]*Optical Communications Research Group, Faculty of Engineering and Environment, Northumbria University, Newcastle-upon-Tyne, NE1 8ST, UK.*

[3]*Department of Electrical and Electronics Engineering, Ozyegin University, Istanbul, Turkey, 34794.*

[nazarzah; xzvanove]@fel.cvut.cz, z.ghassemlooy@northumbria.ac.uk, hossien.eldeeb@ozu.edu.tr, and murat.uysal@ozyegin.edu.tr

***Abstract*—The potential use of flexible substrate-based organic light emitting diodes (OLEDs) as curved or rolled lighting sources offers news opportunities for the implementation of visible light communications (VLC) in indoor environments. This paper outlines the use of such a system in a furnished office and investigates the impact of the beam pattern of OLED, which is symmetrical and wider than Lambertian, on the VLC system. We present new results of the VLC system performance in terms of the root-mean-square delay spread and the bit error rate (BER) for the link using both flat and half-circular OLEDs. We demonstrate a data rate of 4 Mb/s using both the curved and flat OLEDs for the transmitter's half-angle within the range of ±90° and ±53°, respectively with a BER below the forward error correction BER limit.**

Keywords- flexible OLED; visible light communications; bit error rate.

I. INTRODUCTION

In recent years, numerous efforts have been made in modeling the visible light communications (VLC) channel in order to determine the channel impulse response (CIR) and its characteristics in term of the root-mean-square (RMS) delay spread and the average optical path loss (OPL) [1]. The use of organic light emitting diodes (OLEDs) for lighting, TV, etc., has been increasing due to a number of advantages, including transparent displays, rich color, low power consumption and large active areas [2, 3]. However, the low modulation bandwidth B_{mod} (i.e., in the range of hundredth of kHz) of OLEDs is a drawback, which leads to restriction in transmission data rates R_b [3-6].

In [7], Monte Carlo (MC) ray tracing was used to evaluate the CIR of an empty room at the visible wavelength range by considering fixed reflectance values for the surface materials. The first attempt to characterize the VLC channel with wavelength-dependent reflectance was reported in [8], where the authors claimed that, the total diffuse power and the delay spread were lower for VLC compared with the infrared band. In [9], the modified MC ray tracing approach was used for analysing the CIR as a function of the wavelength using a simplified matrix model. Alternatively, a three-dimensional (3D) simulation environment using a CAD software could be adopted to generate 3D vector-type graphics for the VLC system. In [10], a 3D CAD model based on MC algorithm was presented for the VLC system. In [11, 12], a reference channel model-based on Zemax [13] was reported, which was endorsed by the IEEE 802.15.7r1 Task Group. In [14], a VLC channel model was proposed by considering the impact of the dimensions of obstacles within an environment. The point cloud of the obstacle was determined by detecting the received optical rays in photodetector (PD), where every solid angle of the LED illumination area transmit ray by beam steering. In [15], authors claimed that the use of flexible (i.e., curved) OLEDs in VLC systems offer lower RMS delay spread and the average OPL of 8.8% and 3 dB, respectively in comparison with Lambertian source.

This work emphasizes on the evaluation of an attractive feature of OLEDs, which is the mechanically flexible potential for utilizing in VLC system. Our simulation has been presented to find the impact of symmetrical beam pattern of curved OLEDs, which is wider than Lambertian on the VLC channel. In this work, we consider a VLC system in a typical office environment with furniture, where a half-circular OLED, placed on the wall, is acting as a transmitter (Tx). The user, which represents the receiver (Rx), is moving along a circular path at the height of 1 m above the floor level. We investigate the proposed system optical features and show a new numerical model for the RMS delay-spread of the channel. We show that the curved OLED-based VLC link offers improved bit error rate (BER) performance for the angle of radiation > 45° compared with the flat OLED VLC.

The rest of the paper is organized as follows. In Section II, the features of simulation are described. Section III discusses the results. Finally, conclusions are given in Section IV.

II. SIMULATION ENVIRONMENT

The proposed model is composed of three main steps. (*i*) Creating a 3D indoor environment (i.e., an office shown in Fig. 1) considering a specific geometry, imported CAD objects as furniture, types of materials and their reflection coefficients with respect to the wavelength, specifications of the Tx and the Rx. (*ii*) Use of the non-sequential ray tracing to determine the

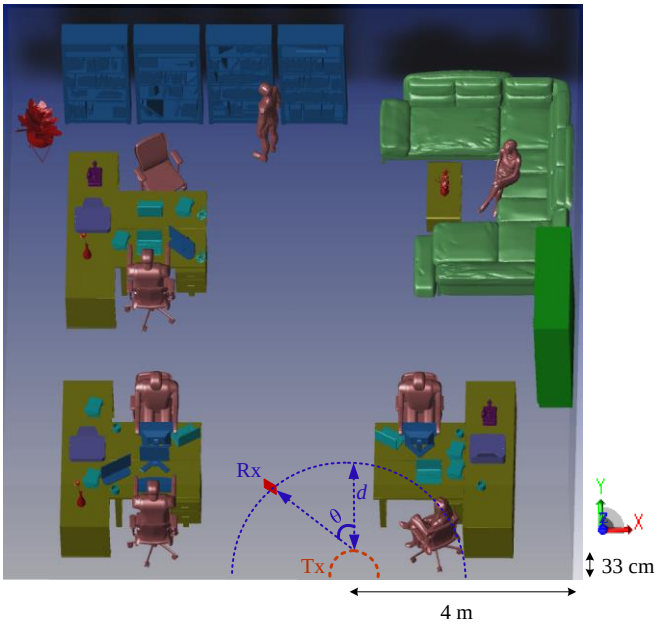

Fig. 1.The three-dimensional indoor environment and proposed scenario which shows the location of Rx and Tx giving a half-circular lighting.

detected optical power and path lengths from the Tx to the Rx. Note, a number of reflections from the floor, ceiling, walls and other objects are considered until the normalized intensity of ray after intercepting an object drops to 10^{-3}. (*iii*) Calculations of CIR, which is carried out by means of importing the captured output data into MATLAB and it is expressed as [11]:

$$h(t) = \sum_{i=1}^{N} P_i \delta(t - \tau_i), \qquad (1)$$

where P_i and τ_i are the power and the propagation time of the ith ray, respectively. δ is Dirac delta function and N is the number of rays received at the Rx.

The spatial intensity distribution of light emitted from the light source is determined by the optical radiation pattern profile. The luminous intensity defined in terms of the angle of irradiance ϕ is given as [16]:

$$I(\phi) = \frac{m_L + 1}{2\pi} I(0) \cos^{m_L}(\phi), \qquad \phi = [-\frac{\pi}{2}, \frac{\pi}{2}] \qquad (2)$$

where $I(0)$ is the center luminous intensity of the OLED and m_L is Lambertian order, which is defined in terms of the Tx semi-angle $\phi_{1/2}$ as [16]:

$$m_L = -\frac{\ln(2)}{\ln[\cos(\phi_{1/2})]}. \qquad (3)$$

In this work, measured characteristics of a flexible OLED from UNISAGA with a size of 200×50 mm^2, see Fig. 2(a), were used as the simulations inputs. The measured beam pattern of the flexible OLED for a half-circular configuration is depicted in Fig. 2(b), showing symmetry but not fitting with Lambertian radiation pattern (the solid line for $m_L = 1$). A close match between the simulated and the measured beam patterns can be seen in Fig. 2(b). The measured spectrum profile of the flexible OLED is presented in Fig. 2(c) showing the red, green and blue components at 620, 553 and 454 and 480 nm, respectively. Fig. 1 shows the location of the OLED and the Rx, which is moving over a semi-circular path of the radius d and an angle of radiation with respect to the normal from the center point of OLED (i.e., -90° < θ < 90°). The Rx height is assumed to be 1 m above the floor to represent people holding mobile phones.

III. Results and Description

The proposed system performance is investigated in terms of the BER for both curved and flat OLEDs. All the key system parameters adopted are given in Table I.

A. Power Distribution on the Rx height level

In order to find the power distribution for both cases; flat and curved OLEDs mounted on the wall, we considered 200 positions for the Rx located on the height of 1 m. As it can be seen in Fig. 3, the maximum power level at the center of the flat OLED is 280 μW, which is higher than 140 μW for the curved OLED. However, for the curved OLED, higher power intensity can be seen for a wider half-angle θ of the Tx. Note, θ = 0° corresponds to the normal from the center point of OLED. E.g., at the Rx's coordinate of (2,1) m, the power values are 40 and 16 μW for the curved and flat OLED, respectively.

(a)

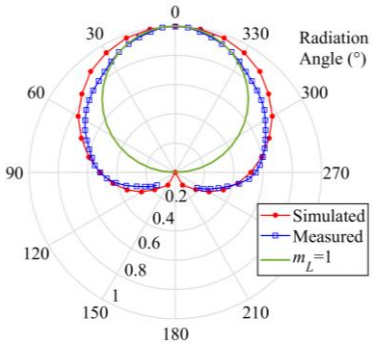

(b)

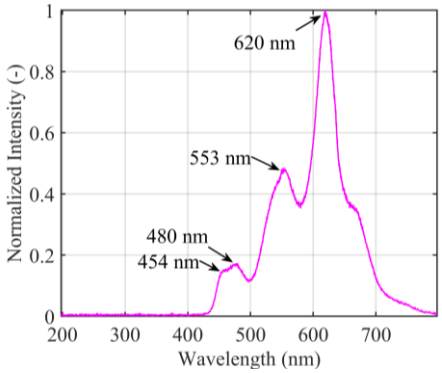

(c)

Fig. 2. The flexible OLED panel and its characteristics adopted in the simulation: (a) photograph, (b) the emission pattern of light source modeled for a curved OLED, which is closely matched with the measured data and (c) the normalized optical spectrum where the peak wavelengths are marked.

TABLE I. THE SYSTEM PARAMETERS

Item	Parameter	Value
Room	Size	10×10×3 m^3
	Type of materials reflections	Purely diffuse
	Maximum reflection order	4
Surface material refractivity in % (RGB)	Chair, sofa (leather)	24, 18.8, 16.3
	Coffee cup (ceramics)	97.1, 96.2, 92.3
	Human clothes (cotton)	67, 58, 45.6
	Plant (leaf)	14, 5.9, 8.2
	Desk, book shelf, book (pine wood)	70, 51, 33.1
	Laptop, PC, printer, and telephone (black gloss paint)	3.4, 3.2, 3.2
Tx	Dimension	1×0.5 m^2
	Type	Flexible
	Bandwidth	50 kHz
	Power of lighting	10 W
	Number of OLED panels	19
	Number of chip/ LED panel	64
	Power of each chip	8.2 mW
	Curvature radius	32 cm
	Location	Fixed on the wall (4, 0.33, 1.5) m
Channel	Length d	2 m
	Time resolution	0.2 ns
Rx	Active area of PD	1 cm^2
	Responsivity	0.4 A/W
	FOV	90°
	Incident angle	0°
	Height	1 m
	One sided noise power spectral density N_o	10^{-19} W/Hz

B. RMS Delay Spread

The delay spread provides a good estimate of how susceptible the channel is to inter-symbol interference (ISI), which leads to reduced R_b. The RMS delay spread is commonly used to define the time dispersion along the propagation path. The channel mean excess delay τ and the RMS delay spread τ_{RMS} are given as [11]:

$$\tau = \frac{\int_0^\infty t \times h(t)dt}{\int_0^\infty h(t)dt}, \tag{4}$$

$$\tau_{RMS} = \sqrt{\frac{\int_0^\infty (t-\tau)^2 \times h(t)dt}{\int_0^\infty h(t)dt}}. \tag{5}$$

Fig. 4 depicts the polar plot of τ_{RMS} for the flat and curved OLEDs. The angle of θ was shown in Fig. 1 identifying the Rx location on the semi-circular path of the radius d. τ_{RMS} increases with θ reaching the maximum value of 5 and 10.7 ns at θ of 90° for curved and flat OLEDs, respectively. It is obvious that, for the curved OLED, there is a slight change in τ_{RMS} by about 0.8 ns with respect to θ. However, τ_{RMS} has changed about 7.3 ns for the flat OLED. Note, there is a significant increase in τ_{RMS} for $\theta > 40°$ for the flat OLED.

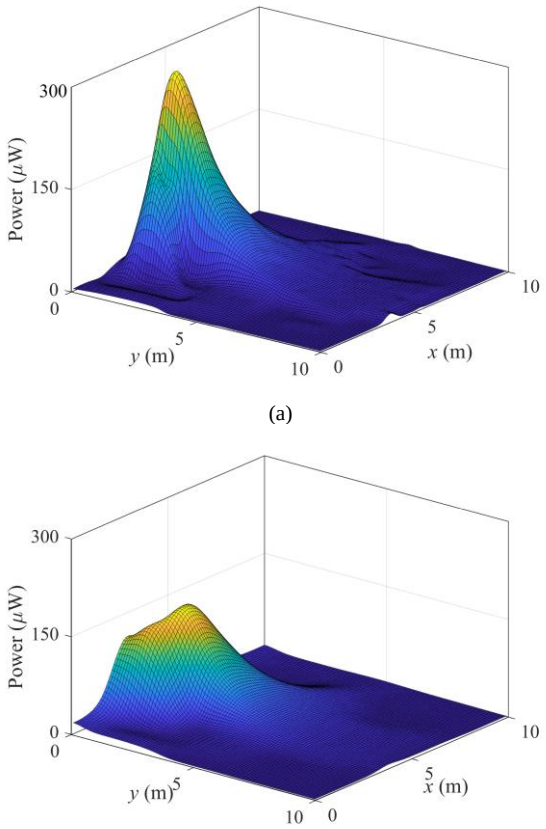

Fig. 3. The power distribution in the case of using: (a) flat OLED and (b) curved OLED.

Using a non-linear approximation algorithms for both cases, a 2-term power series model can be derived from simulations for τ_{RMS} as a function of θ given by:

$$\tau_{\text{RMS}} = p_1\theta^{p_2} + p_3, \tag{6}$$

where p_1, p_2 and p_3 are summarized in Table II. Note, the empirical parameters can vary based on the number of objects in the room and the size of specified confined space.

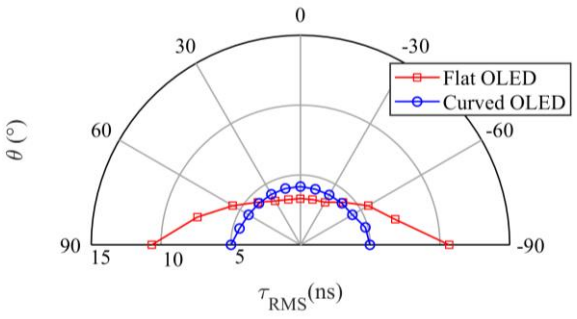

Fig. 4. Comparison of a flat and curved OLEDs employed in the office in term of τ_{RMS}.

TABLE II. NUMERICAL MODELING PARAMETERS FOR τ_{RMS} IN THE CASE OF USING FLAT AND CURVED OLEDS.

OLED type	p_1	p_2	p_3
Curved	8.707×10^{-10}	4.589	4.172
Flat	1.765×10^{-5}	2.875	3.312

C. System Performance

For intensity modulation/direct detection (IM/DD) optical transmission systems, the electrical signal-to-noise ratio (SNR) is defined as [17]:

$$\mathrm{SNR} = \frac{(\gamma P_R)^2}{R_b N_o} = \frac{(\gamma H(0) P_E)^2}{R_b N_o}, \quad (7)$$

where γ is the photodetector's responsivity in (A/W), $H(0)$ is channel DC gain, which defines the achievable SNR, N_o is one-sided power spectral density of the additive white Gaussian noise, and P_E and P_R are the emitted and received optical power, respectively. Considering a channel with non-return-to-zero on-off keying modulation, the BER is given as [17]:

$$\mathrm{BER} = \frac{1}{2} erfc\left(\sqrt{\frac{\mathrm{SNR}}{2}}\right). \quad (8)$$

Fig. 5 shows the polar plots of the BER for flat and curved OLEDs at R_b of 4 and 6 Mb/s along with the 7% forward error correction (FEC) BER limit of 3.8×10^{-3} [18]. Note for 4 Mb/s the BER is below FEC for curved OLED. As illustrated, the BER plot displays a symmetry about the origin (i.e., at θ of 0°) because of the same achievable SNR that is maintained across the entire face of OLED. It is obvious that for the curved OLED the BER is improved over a wider θ compared with the flat OLED. Note, for the flat OLED with $-30° < \theta < 30°$ the BER values are lower than the value of 10^{-6}. At R_b of 4 Mb/s, the BER remains below the FEC limit for θ within the range of $\pm90°$ and $\pm53°$ for the curved and flat OLEDs, respectively. However, for R_b of 6 Mb/s, θ drops by 15° and 4° for the curved and flat OLEDs, respectively.

IV. CONCLUSION

In this paper, we investigated the OLED VLC system performance and the channel characteristics in an office environment. The measured beam pattern profile of the curved OLED was compared with the simulation result showing a close match. We showed that, for the Tx with a half-angle $\theta > 40°$ and using a flat OLED τ_{RMS} increased significantly (i.e., 7.3 ns) compared with 1 ns for the curved OLED. A 2-term power series model was found to match τ_{RMS} as a function of θ. Contrary to the flat OLED, the curved OLED showed improved BER performance over a wider range of θ. A data rate of 4 Mb/s was achieved using both the curved and flat OLEDs for θ within the range of $\pm90°$ and $\pm53°$, respectively.

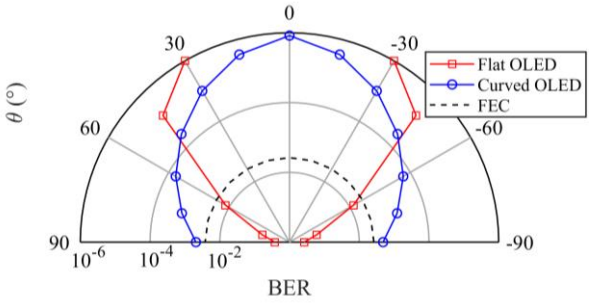

(a)

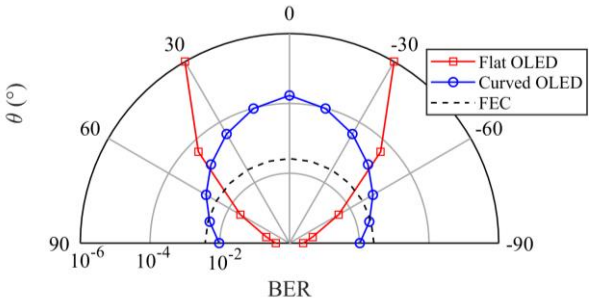

(b)

Fig. 5. The polar plot of BER for flat and curved OLEDs at R_b of (a) 4 Mb/s and (b) 6 Mb/s.

ACKNOWLEDGEMENT

This work is supported by the European Union's Horizon 2020 research and innovation programme under the Marie Sklodowska-Curie grant agreement no 764461 (VISION).

REFERENCE

[1] Z. Ghassemlooy, M.-A. Khalighi, and W. Dehao, "Channel Modeling," in *Visible Light Communications: Theory and Applications*: CRC Press, 2017, pp. 71-92.

[2] J. Kalinowski, *Organic Light-Emitting Diodes: Principles, Characteristics & Processes*. CRC press, 2018.

[3] P. A. Haigh, Z. Ghassemlooy, S. Zvánovec, and M. Komanec, "VLC with Organic Photonic Components," in *Visible Light Communications: Theory and Applications*: CRC Press, 2017, pp. 521-548.

[4] Z. H. Kafafi, *Organic electroluminescence*. CRC Press, 2018.

[5] P. A. Haigh, Z. Ghassemlooy, and I. Papakonstantinou, "1.4-Mb/s white organic LED transmission system using discrete multitone modulation," *IEEE Photonics Technology Letters*, vol. 25, no. 6, pp. 615-618, 2013.

[6] P. A. Haigh *et al.*, "A 1-Mb/s visible light communications link with low bandwidth organic components," *IEEE photonics technology letters*, vol. 26, no. 13, pp. 1295-1298, 2014.

[7] H. Chun, C.-J. Chiang, and D. C. O'Brien, "Visible light communication using OLEDs: Illumination and channel modeling," in *2012 International Workshop on Optical Wireless Communications (IWOW)*, 2012: IEEE, pp. 1-3.

[8] K. Lee, H. Park, and J. R. Barry, "Indoor channel characteristics for visible light communications," *IEEE communications letters*, vol. 15, no. 2, pp. 217-219, 2011.

[9] A. Ramirez-Aguilera, J. Luna-Rivera, V. Guerra, J. Rabadán, R. Perez-Jimenez, and F. J. Lopez-Hernandez, "A generalized multi-wavelength propagation model for VLC indoor channels using Monte Carlo simulation," *Transactions on Emerging Telecommunications Technologies*, vol. 30, no. 2, p. e3490, 2019.

[10] S. P. Rodríguez, R. P. Jiménez, B. R. Mendoza, F. J. L. Hernández, and A. J. A. Alfonso, "Simulation of impulse response for indoor

visible light communications using 3D CAD models," *EURASIP Journal on Wireless Communications and Networking*, vol. 2013, no. 1, p. 7, 2013.
[11] F. Miramirkhani and M. Uysal, "Channel modeling and characterization for visible light communications," *IEEE Photonics Journal*, vol. 7, no. 6, pp. 1-16, 2015.
[12] M. Uysal, F. Miramirkhani, O. Narmanlioglu, T. Baykas, and E. Panayirci, "IEEE 802.15. 7r1 reference channel models for visible light communications," *IEEE Communications Magazine*, vol. 55, no. 1, pp. 212-217, 2017.
[13] Zemax OpticStudio 18.9, [Online]. Available: https://www.zemax.com/products/opticstudio
[14] X. Nan, P. Wang, L. Guo, L. Huang, and Z. Liu, "A novel VLC channel model based on beam steering considering the impact of obstacle," *IEEE Communications Letters*, vol. 23, no. 6, pp. 1003-1007, 2019.
[15] H. Chen and Z. Xu, "OLED panel radiation pattern and its impact on VLC channel characteristics," *IEEE Photonics Journal*, vol. 10, no. 2, pp. 1-10, 2017.
[16] Z. Ghassemlooy, L. N. Alves, S. Zvanovec, and M.-A. Khalighi, *Visible Light Communications: Theory and Applications*. CRC Press, 2017.
[17] P. Pinho, *Optical Communication Technology*. BoD–Books on Demand, 2017.
[18] J. G. Proakis and M. Salehi, *Digital communications*. McGraw-hill New York, 2001.